Bull Earthquake Eng (2009) 7:637–659
DOI 10.1007/s10518-009-9105-x

ORIGINAL RESEARCH PAPER

Ground-motion prediction equations (GMPEs) for inelastic response and structural behaviour factors

R. Rupakhety · R. Sigbjörnsson

Received: 8 October 2008 / Accepted: 22 January 2009 / Published online: 12 February 2009

Abstract The objective of this paper is to present ground-motion prediction equations describing constant-ductility inelastic spectral ordinates and structural behaviour factors. These equations are intended for application within the framework of Eurocode 8. Most of the strong-motion data used in the present work is obtained from the ISESD (Internet Site for European Strong-motion Data) databank. Present analysis includes ground motion records from significant Icelandic earthquakes, which are augmented by records obtained from continental Europe and the Middle East. In all cases the selected ground motion records are generated during shallow earthquakes within a distance of 100 km from the recording station. The classification of site conditions in the present work is based on the Eurocode 8 definition.

Keywords Eurocode 8 · Ground-motion prediction · Attenuation relationship · Structural behaviour factor · Inelastic response · Constant-ductility response spectrum

1 Introduction

Within the framework of Eurocode 8 (European Committee for Standardization 2003), the earthquake motion at a given point on the Earth's free surface is represented by a linear elastic acceleration response spectrum popularly known as elastic response spectrum. Such a spectrum is constructed by scaling a predefined spectral shape with the peak ground acceleration corresponding to the hazard at the given site. Therefore, it is required that probabilistic seismic zoning maps displaying peak ground acceleration for an appropriate mean return period, usually taken as 475 years, are available. Such constant hazard maps are produced by performing probabilistic seismic hazard assessment (Cornell 1968).

For quantifying the seismic hazard at a given site, or for producing a seismic zoning map of a region for generalized applications, it is necessary to establish equations to calculate

R. Rupakhety · R. Sigbjörnsson (✉)
University of Iceland, Earthquake Engineering Research Centre, Austervegur 2a, 800, Selfoss, Iceland
e-mail: Ragnar.Sigbjornsson@hi.is

various strong-motion parameters as a function of earthquake size, distance to source and the geological conditions. Acceleration time-histories, which provide the most comprehensive information about the ground motion, are not feasible to be modelled by empirical equations because their amplitude is stochastic in nature. In the past the usual practice has been to develop an attenuation relation for the peak ground acceleration, which is used to scale a normalized standard spectral shape (e.g. Biot 1942; Housner 1959; Newmark and Hall 1969; Seed et al. 1976; Mohraz 1976). McGuire (1977) pointed out the inadequacy of peak ground acceleration and a fixed spectral shape as a measure of strong motion intensity. Instead he used the maximum response of linear elastic oscillators for defining a ground motion parameter proportional to the maximum response of 1 Hz, 2% damped linear elastic oscillator which in conjunction with the peak ground acceleration was demonstrated to lead to a risk-consistent design spectra. Trifunac (1992) discussed the various factors such as the size of the earthquake source, geologic site conditions, local soil conditions and frequency dependent attenuation that actually influence the variations in spectral shapes. To avoid the use of peak ground acceleration scaled predefined spectral shape several attenuation relations have been developed, for maximum response of linear elastic oscillators at various natural periods, by many investigators in the past (Douglas 2003; Bommer 1998; Ambraseys et al. 2005; Bindi et al. 2006; Berge-Thierry et al. 2003; Cauzzi and Faccioli 2008 to mention a few).

The basis of design according to Eurocode 8 is the inelastic response spectrum of a single degree-of-freedom system exhibiting an elastic-perfectly-plastic force-deformation relation under monotonically increasing loading. Such a system is completely defined by its undamped natural period of vibration (T), damping ratio (ζ) expressed as a percentage of critical value and the yield force (F_y).

Once the elastic response spectrum is developed, Eurocode 8 permits to derive the inelastic response spectrum by applying the so-called structural behaviour factor, q, defined by the following ratio

$$q = \frac{\max |F_{\text{elastic}}|}{F_y} \tag{1}$$

Here, F_{elastic} is the force that would develop if the system behaved as linear-elastic and F_y is the yield force of an inelastic system. The peak displacement demand of the structure is then expressed in terms of the ductility factor defined as follows

$$\mu = \frac{\max |u|}{u_y} \tag{2}$$

where, u_y is the yield displacement of the system and u is the induced displacement. The use of behaviour factor permits the calculation of seismic internal forces required to design the members of structures through linear elastic analysis. In such a procedure Eurocode 8 requires that the structure possesses the capacity to sustain a peak global displacement demand at least equal to its global yield displacement multiplied by the displacement ductility factor corresponding to the q value that was used to reduce the elastic spectral ordinates when deriving the inelastic spectral values.

This procedure could be applied with higher confidence if, instead of reducing the elastic response spectrum with the so-called q factor, the designer had access to uniform hazard spectrum of inelastic response. To construct such uniform hazard spectrum within the framework of probabilistic seismic hazard assessment (PSHA), proper ground-motion prediction equations for inelastic systems need to be developed.

One of the most recent works that have been performed regarding maximum response of inelastic oscillators is that by Tothong and Cornell (2006). They developed attenuation

relationships for the ratio of inelastic spectral displacement to its elastic counterpart. These ratios were used with existing attenuation relationships for elastic spectral displacement (e.g. Abrahamson and Silva 1997) to produce the inelastic displacement spectra. Borzi et al. (2001) established some equations for computing the ratio of elastic spectral displacement to inelastic spectral displacement single degree-of-freedom oscillators. This ratio, termed as the displacement modification factor is, in displacement based design (Moehle 1992; Kowalsky et al. 1994; Priestley et al. 2007) a coefficient equivalent to the behaviour factor in force based design.

As mentioned earlier, a number of attempts have been made to develop inelastic displacement spectra. Such spectra could be easily converted into the pseudo-acceleration spectra simply by multiplying with the square of the natural frequency of vibration. Displacement spectra are useful in performance based design (Priestley 2000; Bertero 1997), structural demand analysis and displacement based design. Within the framework of Eurocode 8, acceleration spectra are the primary requirement and displacement spectra are derived from them. Additionally, we believe that deriving the inelastic spectra from the elastic spectra by using the displacement modification factors or the inelastic displacement ratios as mentioned earlier involves higher uncertainty due to the fact that apart from the uncertainty that is present in the estimation of the elastic response spectrum, an additional uncertainty is added in the final product which is a result of the regression analysis for the empirical equations of the displacement modification factors or the inelastic displacement ratios. The second source of uncertainty could be easily avoided by directly developing empirical equations for the maximum response of inelastic oscillators. This is justified by the results we present later which show that the standard deviation of residuals associated with the prediction of the elastic response and the inelastic response are comparable. In this study we focus on the task of developing GMPEs for constant-ductility response spectral ordinates.

1.1 The study area

The study area of the present work is Iceland, in particular the South Iceland Seismic Zone. The earthquakes in this zone are characterised as shallow, moderate to strong, with a predominant strike-slip faulting mechanism. The fault planes of the largest earthquakes are in all cases close to vertical and the rupture typically propagates to the surface (Sigbjörnsson et al. 2008).

Iceland lies on the diverging boundary of the North American and Eurasian plates, also known as the Mid-Atlantic Ridge. This boundary can be distinguished into regions of active tectonic extension and transformation, respectively. The transform zone of the Mid-Atlantic Ridge is associated with earthquake hazards in Iceland. Regions of the greatest earthquake hazard in Iceland can be broadly divided into the South Iceland Seismic Zone (SISZ) in the south and the Tjornes Fracture Zone (TFZ) in the north. The SISZ covers the largest agricultural area in Iceland and is among its most densely populated regions (Sigbjörnsson et al. 2008). This area has witnessed considerable earthquakes in the past. Here it is especially worth mentioning the following four events: The 6 May 1912 M_w 7 earthquake, the 17 June 2000 M_w 6.5 earthquake, the 21 June 2000 M_w 6.4 earthquake and the 29 May 2008 M_w 6.3 earthquake. The latest earthquake caused widespread damage in the densely populated region near the western border of the SISZ, including the towns of Hveragerdi and Selfoss (Sigbjörnsson et al. 2008).

The SISZ is situated between two sections of the Mid-Atlantic Ridge, i.e. the Reykjanes Peninsula, which is the inland extension of the Reykjanes Ridge, and the Eastern Volcanic

Zone. It is not an ideal transform fault, as it does not connect both rifts at right angles and as the earthquakes do not occur on EW-trending left-lateral shear faults but on their conjugate, NS-oriented right-lateral, rupture planes. This is indicated by surface fault traces and aftershock distributions.

2 Methodologies

2.1 Functional form of the model

The GMPE model for linear elastic as well as constant ductility spectral ordinates used in the present study is the one suggested by Ambraseys et al. (1996) for linear elastic system, which is represented as:

$$\log_{10}(S_a) = b_1 + b_2 M_w + b_3 \log_{10}\sqrt{d^2 + b_4^2} + b_5 S \tag{3}$$

Here, S_a is the spectral ordinate; b_1, b_2, b_3, b_4 and b_5 are the model parameters obtained by regression analysis; M_w is the moment magnitude; d is the distance from the site to the surface trace of the causative fault measured in km; and S is the site factor, which is taken as 0 for rock sites and 1 for stiff soil conditions. Rock sites are classified as Site Class A and stiff soil as Site Classes B and C in the Eurocode 8 provisions. The site classification is based on the average shear wave velocity in the upper 30 m of soil profile at a strain of 10^{-5} or less represented by the symbol $v_{s,30}$ in Eurocode 8. Site Class A is characterized by $v_{s,30} > 800$ m/s; site class B by $360 < v_{s,30} < 800$ m/s and site class C by $180 < v_{s,30} < 360$ m/s .

Many researchers have discussed the magnitude dependence of the far-field decay rate. It has been pointed out that response spectral ordinates induced by larger earthquakes decay slower than those by smaller ones and the decay rate, represented by b_3 in Eq. 3, of smaller sized earthquakes is faster than the commonly assumed -1 (Ambraseys et al. 2005). For a comprehensive review of the possible causes of decay rates faster than -1, readers are referred to Frankel et al. (1990). Ambraseys et al. (2005) observed that the geometric decay rate is magnitude dependent based on their analysis of records from ten earthquakes. Due to the limitation of number of data available, they assumed a linear relationship. As the present study is confined to a much smaller geographic region, less data are available and an attempt to determine the accurate dependence of the decay rate on the magnitude is not believed to produce conclusive results. Therefore, we have assumed a decay rate that is magnitude independent. Boore et al. (1997) introduced a term with quadratic dependence on magnitude in their model to account for the fact that the scaling of ground motion parameters with magnitude is different for events that rupture the entire seismogenic zone. However, Ambraseys et al. (2005) concluded that for shallow crustal earthquakes investigated by them, such an inclusion did not produce significant differences. In this work we do not consider the quadratic dependence of ground motion parameters. Furthermore, due to limitation of data it has been assumed that the anelastic decay is effectively represented by the geometrical spreading parameter, b_3 in Eq. 3.

The structural behaviour factor can be computed as follows

$$q(\mu, T, \zeta) = \frac{S_{\text{elastic}}(T, \zeta)}{S_{\text{inelastic}}(\mu, T, \zeta)} \tag{4}$$

The numerator in the right hand side of Eq. 4 is calculated from the appropriate GMPE (see Eq. 3) where the model parameters are obtained by performing regression analysis on the elastic response spectral ordinates. The denominator is computed by using the GMPE (see Eq. 3) where the model parameters are fitted to the corresponding constant-ductility response spectral ordinates.

2.2 Regression method

Equation 3 suggests that the model being used is non-linear in parameter b_4. Simple multiple linear regression following the method of ordinary least squares, which can be effectively used for linear models (Ambraseys amd Bommer 1991), can not be applied for non-linear models. However, it is clearly understood from the functional form of the model that for a constant value of the model parameter b_4, the model becomes linear and can easily be solved by standard procedure of ordinary least squares regression. The question now arises: Which value of the model parameter b_4 is realistic for the dataset being used? To answer this question we adopt an iterative procedure. Since the parameter b_4 represents a depth parameter, we know that it has a finite positive value. Therefore we start with a value of b_4 equal to 0 and make the model linear. The least square solution of such a model will result in certain value of the standard deviation of the residuals. Then the value of parameter b_4 is increased in small increments and standard deviation of residuals calculated for each corresponding value of the parameter b_4. Since we are basically dealing with shallow earthquakes we increase the value of b_4 to 10 km. The value of b_4 that results in the lowest value of standard deviation of the residuals is adopted. It can easily be seen that minimizing the standard deviation of the residuals is actually equivalent to minimizing the sum of squares of the deviation of predicted response from its observed value.

3 Data applied

The strong-motion records used in the present work are listed in the Appendix, Table 1. The records are primarily those obtained from South Iceland but are augmented by data from continental Europe and the Middle East. The data for the first 76 recordings in Table 1 are obtained from the CD entitled European Strong-Motion Database, Vol. 2 (Ambraseys et al. 2004b). The data for recordings 76–82 in Table 1 are obtained from the Internet Site for European Strong-Motion Data (ISESD) databank (Ambraseys et al. 2004a). Records 83–93 in Table 1 were generated during the 29 May 2008 Iceland earthquake. The corrected acceleration time histories for these records were obtained from the ICEARRAY strong-motion array. ICEARRAY is a small-aperture strong-motion array in South Iceland consisting of 15 strong-motion recording stations situated in the town of Hveragerdi (Sigbjörnsson et al. 2008). A total of 186 strong-motion acceleration time histories (two horizontal components for each of the 93 recording stations listed in Table 1) have been used in the present work.

3.1 Magnitude

The magnitude scale used is the moment magnitude M_w proposed by Kanamori (1977). The records are generated by earthquakes varying in magnitude from 5 to 7.7.

3.2 Source-to-site distance

The distance parameter used in the present work is the distance to the surface projection of the fault (Joyner and Boore 1981), commonly known as fault distance. In cases where the fault distance is not available, epicentral distance is used instead. These distances were obtained from Ambraseys et al. (2004a,b) except for the ICEARRAY recordings. For the ICEARRAY recordings, epicentral distances were computed based on the macroseismic epicentre of 63.98°N and 21.13°W (Sigbjörnsson et al. 2008). The records show a variation in fault distance from 1 to 97 km. Recordings further away from the fault are excluded as they are believed to be of low engineering significance. Such an approach also reduces the difference in anelastic decay in different regions of Europe and the Middle East (Ambraseys et al. 2005).

3.3 Faulting mechanism

Most of the records are generated during strike slip earthquakes except for the recordings from the 1998 Iceland earthquake (records 70–76 in Table 1). Although this earthquake is characterized with oblique faulting mechanism, the fault plane is nearly vertical and the relative motion of the fault planes is predominantly in the direction of the strike.

3.4 Building type

It is believed that the ground motion characteristics of strong-motion records are altered by properties of large buildings, where the recording instruments are commonly stored. Due to limited availability of data, such records were not omitted. However, records from the June 2000 Iceland earthquake, and 29 May 2008 Iceland earthquake which were recorded at the Thjorsarbru Bridge, have been omitted because they show distinct structural influences and site dependent conditions not characteristic of the study area as a whole.

3.5 Site conditions

The criteria based on classifying the site are within the framework of Eurocode 8. Only those sites that are classified as Site Class A, B or C are included in the analysis. Soft soil data have been neglected because they are not characteristic of the study area. Although the recordings from the December 1990 Armenia earthquake satisfy all of the criterion for record selection discussed above, they have been excluded due to the fact that they are characterized by non-extensional region which is not characteristic of the study area.

3.6 Data correction

The acceleration time histories available in Ambraseys et al. (2004a,b) were obtained in corrected form. Data obtained from the ICEARRAY recordings were corrected by using band pass filters with individually chosen cut-off frequencies.

3.7 Spectral amplitudes

The elastic response spectra are computed from the corrected time histories corresponding to 66 log-spaced undamped natural periods in the range 0.04–2.5 s. Inelastic spectra

are computed assuming an elastic-perfectly-plastic force-displacement relation of a single degree-of-freedom oscillator characterized by an undamped natural period, ductility factor and a damping ratio of 5% of the critical. The computations are performed using the software Bispec version 1.61 (Hachem 2000, 2008) and reconfirmed with the results obtained from the software SeismoSignal (SeismoSignal 2007). The time step of integration was set to the minimum of the sampling time of the acceleration time history and the natural period divided by 20. Out of the spectral acceleration corresponding to the two horizontal components, the larger value is selected.

4 Results

The results of the regression analysis are displayed in Fig. 1. The values of the model parameters and the standard deviation of the residuals are listed in Appendix Tables 2, 3, 4, 5 for selected natural periods. It is seen that the estimated model parameters are not smooth functions of the undamped natural period, but apparently possess some irregularities or randomness. The standard deviation of the residuals obtained for the model is comparable to what has been reported in the literature for elastic response spectral ordinates (see Douglas 2003).

Figure 2 shows the comparison of the model with the observed peak ground acceleration (PGA). Figures 3 and 4 show the comparison of the capacity demand for elastic as well as inelastic structures computed by the proposed model to the observed values for natural periods of 0.2 and 1.0 s respectively. Careful examination of Figs. 2 and 3 shows that the scatter of the observed capacity demand around the predicted values is comparable for linear

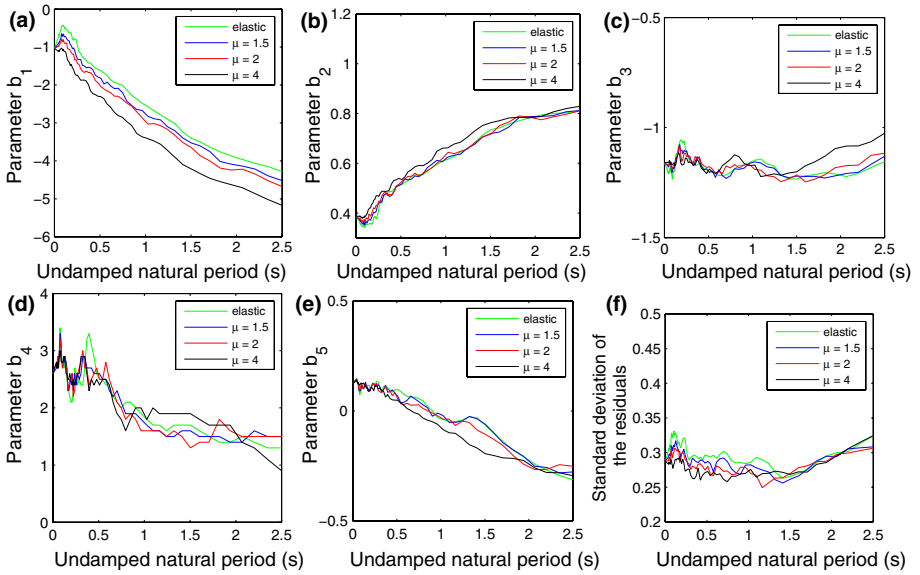

Fig. 1 Model parameters and corresponding standard deviation of residuals for the regression model of Eq. 3. The parameters are obtained both for linear elastic systems and inelastic systems with ductility ratio equal to 1.5, 2.0 and 4.0, respectively. Damping ratio is 5% of critical in all cases

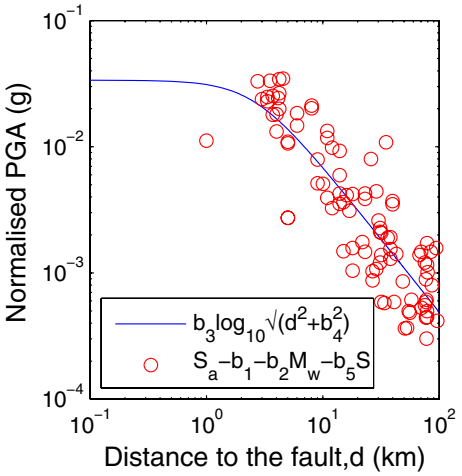

Fig. 2 Comparison of the proposed model with the observed PGA values. The solid blue line corresponds to the result of the proposed GMPE and the red circles are the observed values. Note that the vertical axis has been normalized

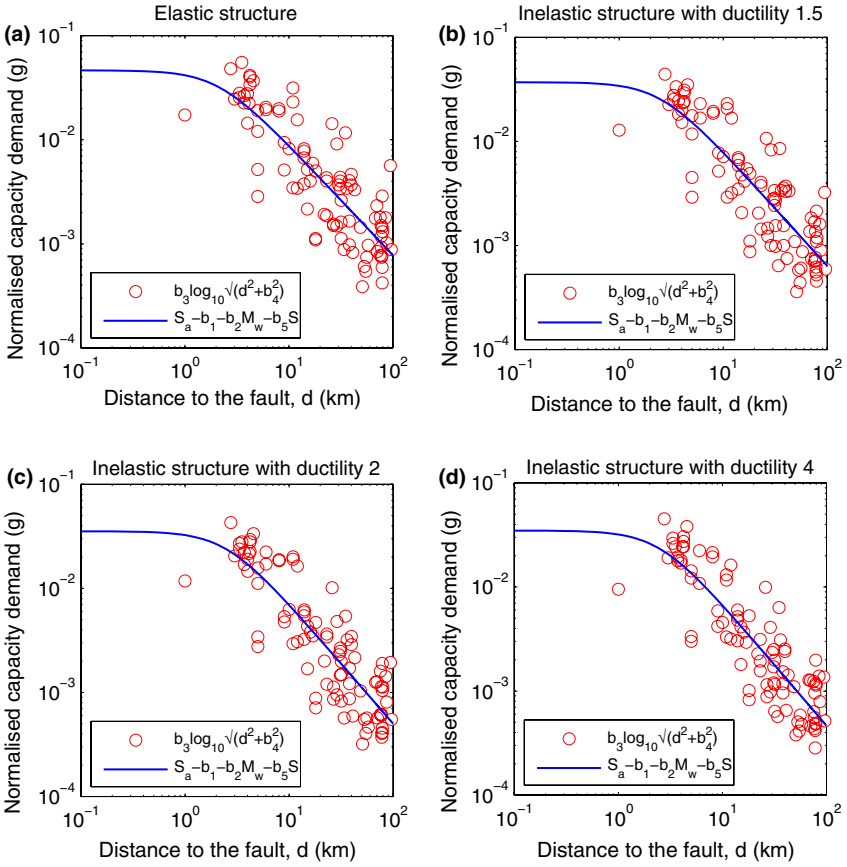

Fig. 3 Comparison of the capacity demand estimated by the proposed model to the observed values for natural period of 0.2 s and damping 5% of critical. The solid blue line corresponds to the result of the proposed GMPE and the red circles are the observed values. Note that the vertical axis has been normalized

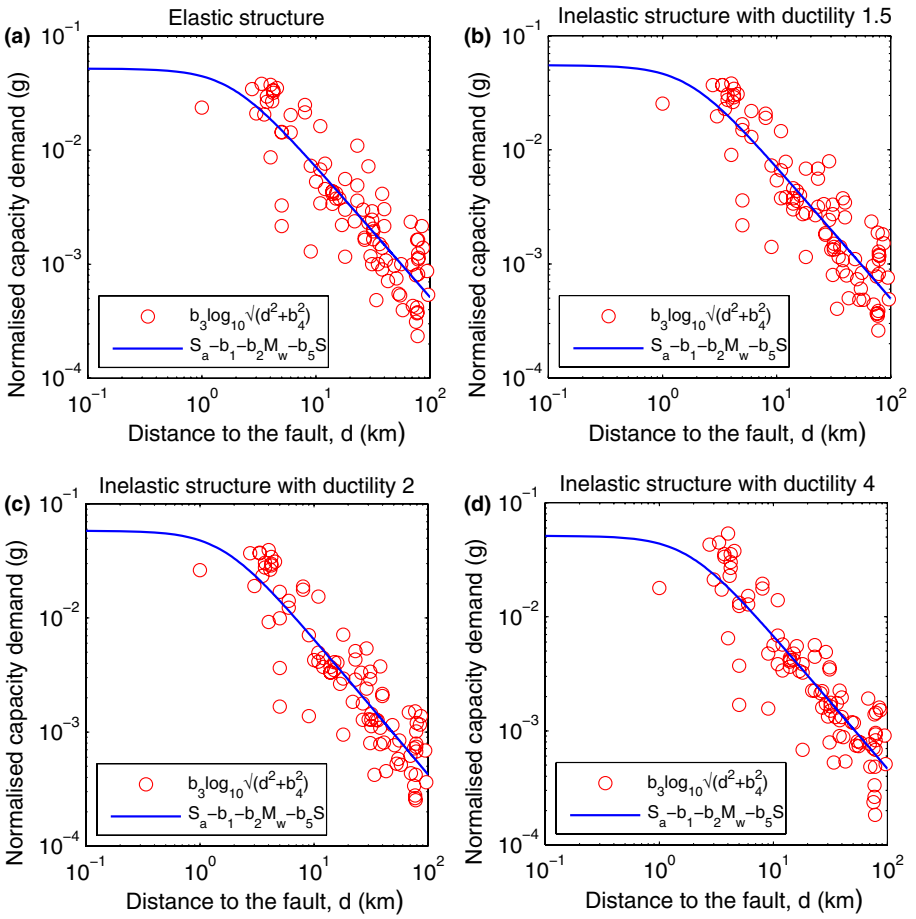

Fig. 4 Comparison of the capacity demand estimated by the proposed model to the observed values for natural period of 1 s and damping 5% of critical. The solid blue line corresponds to the result of the proposed GMPE and the red circles are the observed values. Note that the vertical axis has been normalized

elastic structures and for inelastic structures having ductilities 1.5, 2 and 4. This justifies the assumption that the functional form of Eq. 3 proposed by Ambraseys et al. (1996) for linear elastic systems is equally valid for inelastic structures too.

Selected spectral ordinates representing capacity demand are plotted in Fig. 5 as a function of fault distance. The capacity demand decreases with increasing distance as expected. Furthermore, stiff soil requires a higher capacity demand than rock site and so do stiff structures ($T = 0.2$ s) compared to the more flexible ones ($T = 1.0$ s). The corresponding structural behaviour factors are presented in Fig. 6. It is seen that the ductility value, equal to 1.5, yields a structural behaviour factor almost equal to 1.5, which is in accordance with Eurocode 8. On the other hand, the structural behaviour factor tends to be smaller for stiff structures ($T = 0.2$ s) than anticipated by Eurocode 8, e.g. for a ductility factor equal to 4.0 the structural behaviour factor varies from 2.5 to 3.5 and for a ductility factor equal to 2, the structural behaviour factor varies from 1.75 to 2.25. For a flexible structure ($T = 1.0$ s), and ductility factors of

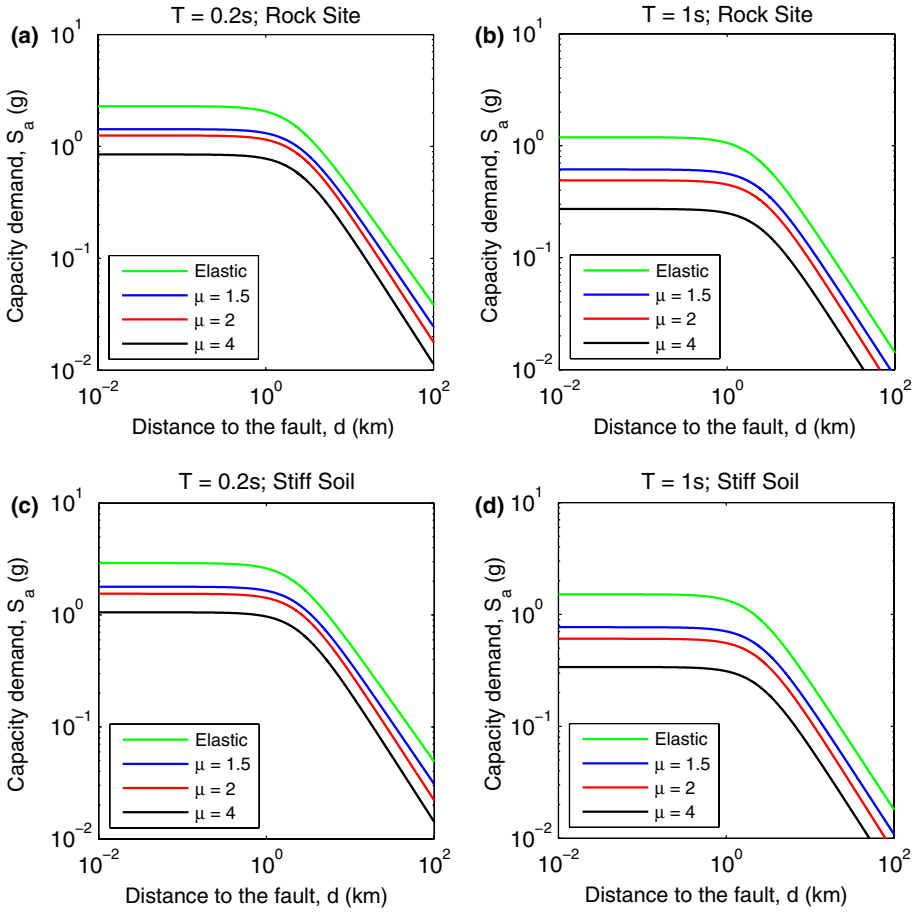

Fig. 5 Capacity demand as a function of distance to fault. Moment magnitude is kept equal to 6.5. Unsmoothed model parameters presented in Fig. 1 are used in producing these figures

1.5 and 2, structural behaviour factors are higher than the Eurocode 8 recommendations; however, for a ductility factor of 4, the structural behaviour factor is smaller than 4.

Figure 7 shows the elastic/inelastic spectra and the structural behaviour factors for a moment magnitude 6.5 earthquake at a distance of 1 km from the fault. It is evident from Fig. 7 that the spectra are jagged, reflecting the irregularities observed in the estimates of the model parameters (see Fig. 1). This is an undesirable feature in general and a smoother spectrum is more attractive for practical purposes. To achieve a smoother spectrum, two approaches were tested. In the first approach the model parameters were smoothed using the Savitzky-Golay procedure (Savitzky and Golay 1964) with a span of 19 and a polynomial of second degree. For the smoothed parameters, the standard deviation of the residuals was recalculated. The results are presented in Fig. 8. In the second approach, the inelastic spectrum itself was smoothed by using a similar procedure (see Fig. 9). It is found desirable to have the model parameters smoothed rather than to smooth the spectrum for each magnitude or distance to the fault. In such a way, the GMPE can be directly used to obtain a reasonably

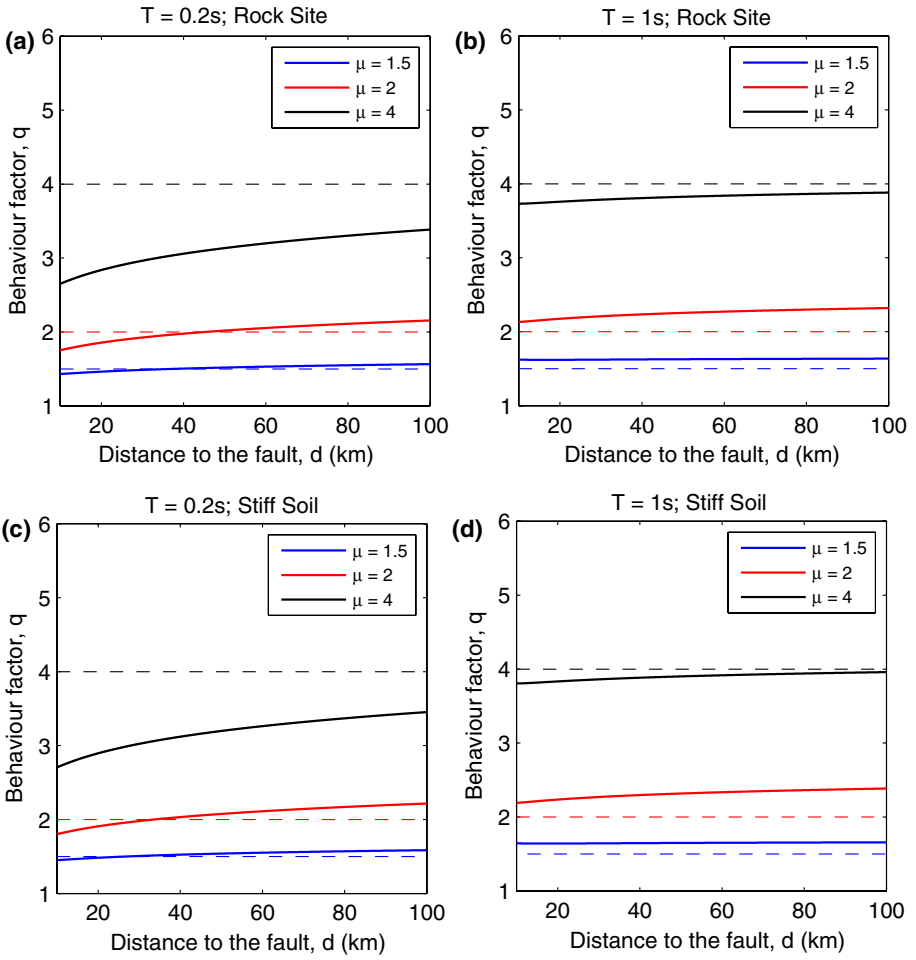

Fig. 6 Structural behaviour factor as a function of distance to fault. Moment magnitude is kept equal to 6.5. Unsmoothed model parameters presented in Fig. 1 are used in producing these figures. The solid lines represent the results of the present study and the dashed lines are the Eurocode 8 recommendations

smooth spectrum. On the other hand, it is necessary to verify that the smoothing of model parameters does not disturb the inherent correlation between the model parameters (if any). To explore this we have calculated the correlation matrix of the original unsmoothed parameters obtained by regression and compared with the correlation matrix of the parameters obtained after smoothing. For elastic structures the correlation matrices before and after smoothing are respectively equal to

$$\begin{bmatrix} 1 & -1 & 0.33 & 0.86 & 0.92 \\ -1 & 1 & -0.34 & -0.84 & -0.9 \\ 0.33 & -0.34 & 1 & 0.02 & 0.27 \\ 0.86 & -0.84 & 0.02 & 1 & 0.81 \\ 0.92 & -0.9 & 0.27 & 0.81 & 1 \end{bmatrix} \quad \text{and}$$

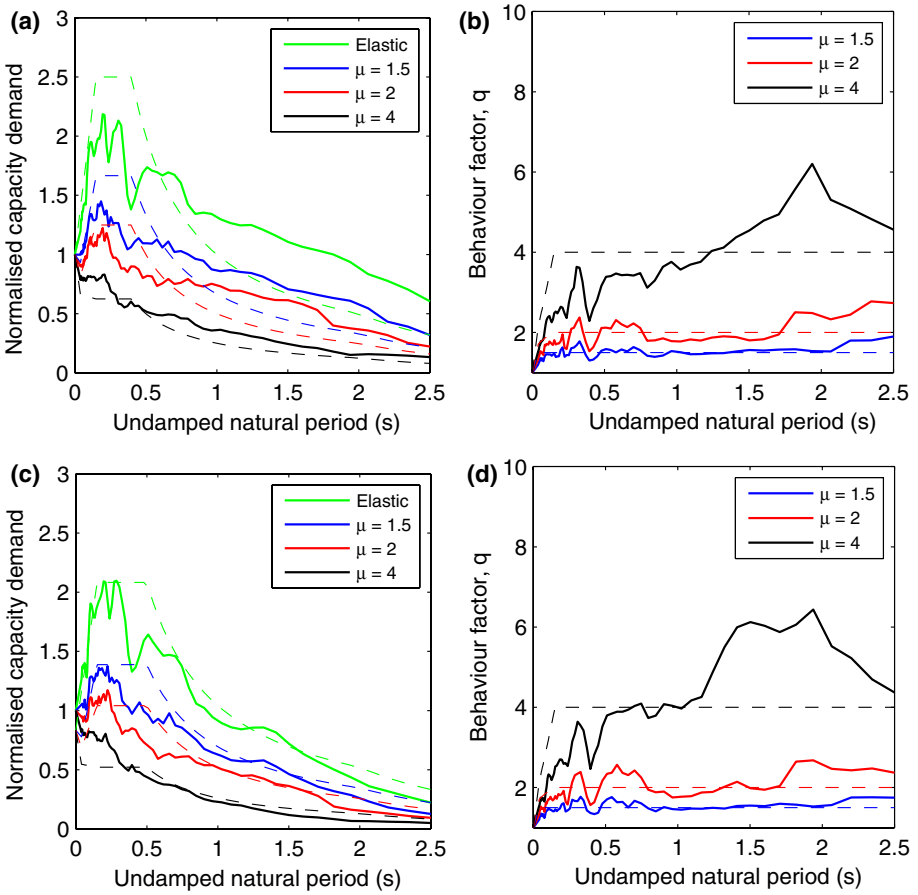

Fig. 7 Inelastic spectrum and structural behaviour factor for a magnitude 6.5 earthquake, at a site where distance to fault is 1 km. Unsmoothed model parameters presented in Fig. 1 are used to produce these figures. **a** and **b** correspond to the rock site and **c** and **d** correspond to the stiff soil site. The solid lines are results of the proposed GMPEs and the dashed lines are the Eurocode 8 recommendations

$$\begin{bmatrix} 1 & -1 & 0.34 & 0.89 & 0.92 \\ -1 & 1 & -0.35 & -0.87 & -0.91 \\ 0.34 & -0.35 & 1 & 0.03 & 0.29 \\ 0.89 & -0.87 & 0.03 & 1 & 0.83 \\ 0.92 & -0.91 & 0.29 & 0.83 & 1 \end{bmatrix}.$$

It can be observed that the correlation between the model parameters is not greatly altered by the smoothing procedure. Similar behaviour was observed for ductile inelastic structures. It can be seen by comparing the standard deviation of residuals from Figs. 1f and 8f that the smoothing procedure does not result in any significant change in the standard deviation of the residuals. Figure 9 presents the comparison of the spectra computed by using the smoothed parameters of Fig. 8 with the Eurocode 8 recommendations.

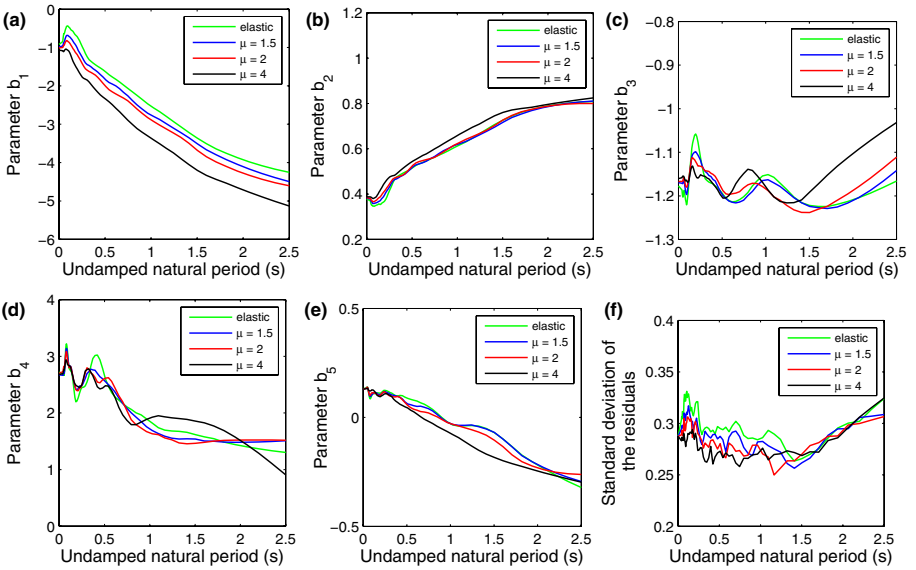

Fig. 8 Smoothed model parameters and corresponding standard deviation of residuals for the regression model of Eq. 3

5 Discussion and conclusions

The correlation matrix of the model parameters indicates that model parameters are highly correlated. This reflects a strong multi-collinearity; a condition that implies imprecise estimates of the regression coefficients. However, the fitted model may still be useful. In such cases, interpolations in the original space of the predictors are satisfactory and the standard deviation of the residuals is reasonably small, which is the case as seen in Figs. 1f and 8f. This implies that while the individual parameters may be poorly estimated, the function represented by the model is estimated fairly accurately. However, it should be pointed out that extrapolation of the model outside the data region of independent variables, i.e. magnitude and distance, used in this study could possibly lead to unreliable results.

We have observed that smoothing of the regression parameters in a model as such is found to be desirable. It is noticed that smoothing of the model parameters, despite of not causing any significant changes in the standard deviation of the residuals, resulted in a fairly smooth spectrum.

It is observed by investigating the Appendix Table 2 (see also Fig. 1) that the parameter b_3 is in the range -1.23 to -1.06 for linear elastic structures. Furthermore, for inelastic systems it is observed that the b_3 parameter is in a similar range but with a tendency towards decreasing attenuation with increasing ductility (see Appendix Table 3, Table 4 and Table 5). In general it is found that the attenuation revealed by this study is comparable with the values obtained by Ambraseys et al. (2005) for magnitude values in the range 6–6.5, but contradicts the fast attenuation indicated by studies dealing with individual earthquakes in the South Iceland Seismic Zone (Sigbjörnsson and Ólafsson 2004; Sigbjörnsson et al. 2007, 2008). However, a regression procedure similar to that used in this present study when applied to the 17 records generated during the 29 May 2008 earthquake resulted in the values of the parameters b_3 and b_4 equal to -1.87 and 6.4, respectively. These observations

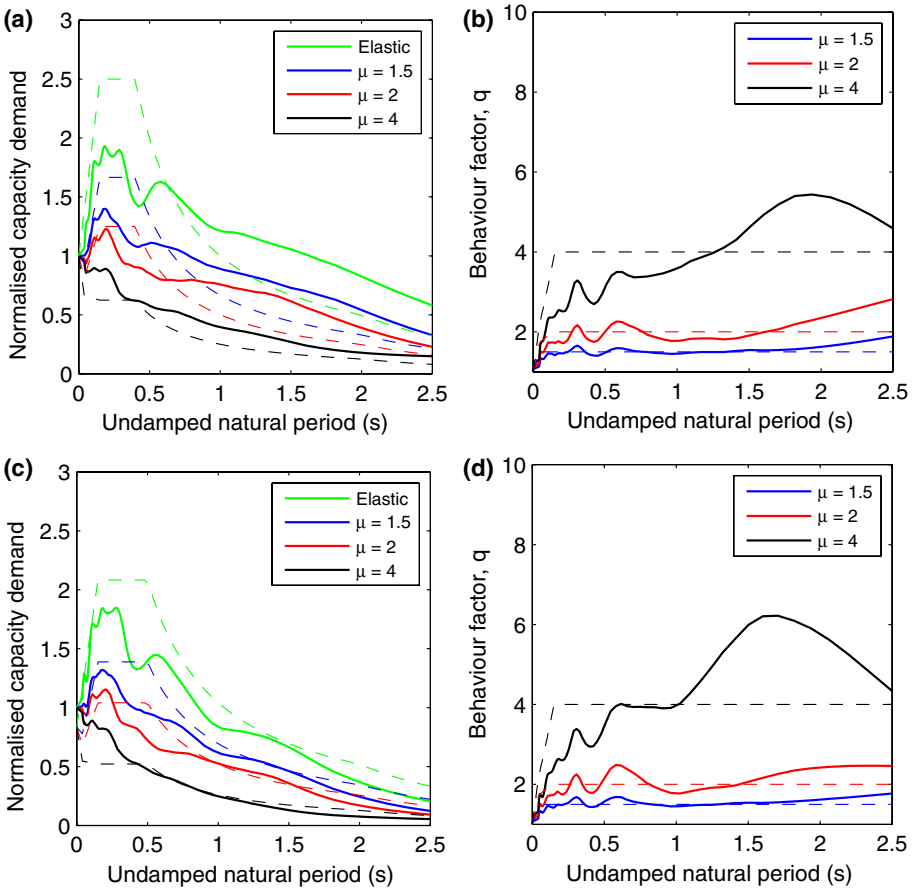

Fig. 9 Comparison of the spectra computed by using the smoothed model parameters of Fig. 8 with the Eurocode 8 recommendations. The solid lines represent the results of the present work and the dashed lines represent the Eurocode 8 recommendations. **a** and **b** are for rock site and **c** and **d** are for stiff soil sites. The moment magnitude is taken equal to 6.5 and the distance to the fault is 1 km

are in close agreement to the depth parameter of 6.2 km and attenuation proportional to the inverse of the squared distance as reported by Sigbjörnsson et al. (2008). This indicates a faster attenuation of the ground motion in the South Iceland region, however, a definite conclusion based on this study alone is not feasible due to the limited number of records available.

The comparison of the spectra computed by the proposed model and the recommendations of Eurocode 8, which is shown in Fig. 7, is interesting to analyze. It should be noted that the Eurocode 8 spectra for inelastic systems are computed based on the assumption that the structural behaviour factor is equal to the ductility factor. It is observed that for elastic structures on rock sites the Eurocode 8 recommendations are conservative for structures having periods less than about 0.6 seconds. However, for flexible structures on rock sites, Eurocode 8 recommendation is seen to under-estimate the spectral ordinates even for elastic structures. This illustrates the limitations of a fixed spectral shape scaled to the peak ground acceleration. For structures designed for target ductilities of 1.5 and 2, the Eurocode 8 recommendations are in good match with the results of the present work especially for stiff structures. How-

ever, for structures with design ductility of 4, the Eurocode 8 recommendation seems to under-estimate the capacity demand on structures located at rock sites for almost whole spectral range considered in the present work.

For stiff soil sites which are classified as site class B and C in Eurocode 8, the soil factor of 1.2 recommended for site Class B is adopted. It is observed that Eurocode 8 recommendations for stiff sites tend to over-estimate the spectral accelerations for structures with higher lateral strength and stiffness. However, as the design ductility is increased to 4, the Eurocode recommendations are under-estimating the capacity demand especially for structures having natural period less than 0.5 s. Another observation worth noticing is that the assumption of adopting structural behaviour factor recommended in Eurocode 8 provisions is not conservative, especially for stiff structures designed for higher values of ductility factors. We observe from Fig. 6 that the structural behaviour factor does not depend significantly on source to site distance. However, it is observed that Eurocode 8 recommendations seem to yield higher values of structural behaviour factor, especially for stiff structures located close to the fault for relatively strong structures. For stiff structures, and a ductility factor of 4, Eurocode 8 recommendations seem to significantly overestimate structural behaviour factor. This implies that stiff structures close to the fault and structures designed assuming higher values of ductility factor will possess inadequate lateral strength. Based on these observations we conclude that the structural behaviour factors to be used in the study area can deviate significantly from the code provisions.

Examination of the standard deviation of residuals in Fig. 1 clearly reveals that the uncertainty involved in prediction of inelastic response is for all practical purposes similar to that involved in the prediction of linear elastic response. This observation forms a strong basis for the development of GMPEs as those proposed in this study for inelastic response. We believe that incorporation of such equations in the framework of PSHA can result in more accurate prediction of peak response of inelastic structures.

Acknowledgements The authors acknowledge the support from the University of Iceland Research Fund. Furthermore we are thankful to the reviewers for constructive criticism. Especially, the authors thank Dr. John Douglas for many comments that resulted in several improvements.

Appendix

Table 1 The earthquake data set used in the present study (WID represents waveform identification within ISESD databank and station identification for ICEARRAY)

SN	Date	Country	Station	M_w	Distance (km)	Site Class	WID
DATA SOURCE: ESMD VOL 2 CD (Ambraseys et al. 2004b)							
1	26.08.1983	Greece	Ouranoupolis seismograph station	5.2	11	A	1917
2	26.08.1983	Greece	Poligiros-Perfecture	5.2	35	A	2027
3	26.04.1997	Greece	Kyparrisia-Agriculture Bank	5.02	26	A	5824
4	12.04.1998	Slovenia	Cerknica	5.7	79	A	6237
5	12.04.1998	Slovenia	Sleme	5.7	97	A	6239
6	04.06.1998	Iceland	Hveragerdi-Church	5.45	6	A	5079

Table 1 continued

SN	Date	Country	Station	M_w	Distance (km)	Site Class	WID
7	04.06.1998	Iceland	Irafoss-Hydro-electric Power Station	5.45	15	A	5085
8	04.06.1998	Iceland	Selfoss Hospital	5.45	18	A	5078
9	04.06.1998	Iceland	Oseyrarbru	5.45	18	A	5090
10	04.06.1998	Iceland	Reykjavik-Heidmork	5.45	23	A	5089
11	04.06.1998	Iceland	Reykjavik-Foldaskoli	5.45	27	A	5088
12	04.06.1998	Iceland	Reykjavik-Hus Verslunarinar	5.45	32	A	5087
13	17.08.1999	Turkey	Izmit-Meteoroloji	7.64	5	A	1231
14	17.08.1999	Turkey	Gebze-Tubitak Marmara Arastirma Merkezi	7.64	30	A	1228
15	17.08.1999	Turkey	Ypai-Kredi Plaza Levent	7.64	77	A	1256
16	17.08.1999	Turkey	Istanbul-Maslak	7.64	78	A	4341
17	17.06.2000	Iceland	Flagbjarnarholt	6.57	5	A	4674
18	17.06.2000	Iceland	Minni-Nupur	6.57	10	A	4675
19	17.06.2000	Iceland	Selfoss Hospital	6.57	31	A	6262
20	17.06.2000	Iceland	Selfoss-City	6.57	31	A	4678
21	17.06.2000	Iceland	Irafoss-Hydro-electric Power Station	6.57	32	A	6269
22	17.06.2000	Iceland	Ljosafoss-Hydro-electric Power Station	6.57	32	A	6270
23	17.06.2000	Iceland	Hveragerdi-Retirement House	6.57	40	A	4679
24	17.06.2000	Iceland	Hveragerdi-church	6.57	40	A	6278
25	17.06.2000	Iceland	Sultartanga-Hydroelectric Power Station	6.57	38	A	6272
26	17.06.2000	Iceland	Hrauneyjafoss-Hydroelectric Power Station	6.57	56	A	6266
27	17.06.2000	Iceland	Reykjavik-Heidmork	6.57	68	A	6276
28	17.06.2000	Iceland	Reykjavik-Foldaskoli	6.57	70	A	6275
29	17.06.2000	Iceland	Reykjavik-Hus Verslunarinar	6.57	76	A	6274
30	21.06.2000	Iceland	Thjorsartun	6.49	3	A	6332
31	21.06.2000	Iceland	Selfoss Hospital	6.49	14	A	6326
32	21.06.2000	Iceland	Selfoss-City Hall	6.49	14	A	6335
33	21.06.2000	Iceland	Irafoss-Hydro-electric Power Station	6.49	14	A	6341
34	21.06.2000	Iceland	Ljosafoss-Hydro-electric Power Station	6.49	15	A	6342
35	21.06.2000	Iceland	Flagbjarnarholt	6.49	22	A	6331
36	21.06.2000	Iceland	Hveragerdi-Church	6.49	23	A	6327
37	21.06.2000	Iceland	Hveragerdi-Retirement House	6.49	23	A	6336

Table 1 continued

SN	Date	Country	Station	M_w	Distance (km)	Site Class	WID
38	21.06.2000	Iceland	Minni-Nupur	6.49	27	A	6333
39	21.06.2000	Iceland	Reykjavik-Heidmork(Jadar)	6.49	51	A	6348
40	21.06.2000	Iceland	Reykjavik-Foldaskoli	6.49	53	A	6347
41	21.06.2000	Iceland	Sultartanga-Hydroelectric Power Station	6.49	55	A	6344
42	21.06.2000	Iceland	Reykjavik-Hus Verslunarinar	6.49	58	A	6346
43	21.06.2000	Iceland	Sigulduvirkjun Hydroelectric Power Station	6.49	78	A	6343
44	26.08.1983	Greece	Ierissos-Police Station	6.71	76	B	2019
45	26.08.1983	Greece	Ierissos-Police Station	5.2	4	B	1882
46	30.10.1983	Turkey	Horasan-Meteo-roloji Mudurlugu	6.63	17	B	354
47	18.05.1988	Greece	Valsamata-Seis-mograph Station	5.84	29	B	947
48	13.03.1992	Turkey	Erzincan-Meteo-rologij Mudurlugu	6.71	1	B	535
49	17.08.1999	Turkey	Gebze-Arcelik	7.64	38	B	1248
50	17.08.1999	Turkey	Goynuk-Devlet Hastanesi	7.64	31	B	1229
51	17.08.1999	Turkey	Istanbul-Bayindir-lik ve Iskan Mudurlugu	7.64	71	B	1218
52	17.08.1999	Turkey	Bursa-Sivil Savunma Mudurluga	7.64	79	B	1216
53	17.08.1999	Turkey	Istanbul-Mecidiyekoy	7.64	77	B	4340
54	17.08.1999	Turkey	Yesilkoy-Havaalani	7.64	87	B	1253
55	17.08.1999	Turkey	Cekmece-Kucuk	7.64	94	B	1252
56	17.06.2000	Iceland	Kaldarholt	6.57	6	B	6263
57	17.06.2000	Iceland	Hella	6.57	5	B	4673
58	17.06.2000	Iceland	Solheimar	6.57	14	B	4676
59	21.06.2000	Iceland	Solheimar	6.49	4	B	6334
60	21.06.2000	Iceland	Kaldarholt	6.49	12	B	6328
61	21.06.2000	Iceland	Hella	6.49	16	B	6330
62	17.08.1999	Turkey	Yarimca-Petkim	7.67	5	C	1257
63	17.08.1999	Turkey	Iznik-Karayollari Sefligi Muracaati	7.67	29	C	1230
64	17.08.1999	Turkey	Bursa-Tofa Fabrikasi	7.67	77	C	1251
65	17.08.1999	Turkey	Fatih-Tomb	7.67	79	C	1254
66	17.08.1999	Turkey	Istanbul-K.M.Pasa	7.67	79	C	6918
67	17.08.1999	Turkey	Istanbul-Zeytinburnu	7.67	80	C	4343
68	17.08.1999	Turkey	Duzce-Meteoroloji Mudurlugu	7.67	12	C	1226

Table 1 continued

SN	Date	Country	Station	M_w	Distance (km)	Site Class	WID
69	17.08.1999	Turkey	Istanbul-Atakoy	7.67	85	C	4337
70	13.11.1998	Iceland	Hveragerdi-Church	5.16	9	A	5028
71	13.11.1998	Iceland	Thorlakshofn	5.16	11	B	5030
72	13.11.1998	Iceland	Oseyrarbru	5.16	11	A	5038
73	13.11.1998	Iceland	Selfoss-Hospital	5.16	18	A	5027
74	13.11.1998	Iceland	Reykjavik-Hus Verslunarinar	5.16	34	A	5035
75	13.11.1998	Iceland	Kaldarholt	5.16	43	B	5029
76	13.11.1998	Iceland	Hella	5.16	49	B	5031
DATA SOURCE: ISESD website (Ambraseys et al. 2004a)							
77	29.05.2008	Iceland	Reykjavik-Fold-askoli	6.3	41	A	13005
78	29.05.2008	Iceland	Hella	6.3	36	A	13007
79	29.05.2008	Iceland	Reykjavik-Heidm-ork(Jadar)	6.3	38	A	13008
80	29.05.2008	Iceland	Ljosafoss-Hydro-electric Power Station	6.3	9	A	13009
81	29.05.2008	Iceland	Selfoss- City Hall	6.3	8	A	13010
82	29.05.2008	Iceland	Selfoss-Hospital	6.3	8	A	13011
DATA SOURCE: ICEARRAY							
83	29.05.2008	Iceland	Heidarbrun	6.3	2.75	A	IS601
84	29.05.2008	Iceland	Kambahraun	6.3	4.56	A	IS602
85	29.05.2008	Iceland	Dynskogar	6.3	4.15	A	IS603
86	29.05.2008	Iceland	Borgarhraun	6.3	4.2	A	IS604
87	29.05.2008	Iceland	Borgarhraun	6.3	4.23	A	IS605
88	29.05.2008	Iceland	Arnarheidi	6.3	4.22	A	IS607
89	29.05.2008	Iceland	Sunnumork(E)	6.3	3.33	A	IS608
90	29.05.2008	Iceland	Sunnumork(W)	6.3	3.33	A	IS688
91	29.05.2008	Iceland	Dvalarheimilid As	6.3	3.74	A	IS609
92	29.05.2008	Iceland	Reykir	6.3	3.52	A	IS610
93	29.05.2008	Iceland	Heidmork	6.3	3.71	A	IS611

Table 2 Model parameters for linear elastic structure

T	b_1	b_2	b_3	b_4	b_5	σ
PGA	−1.038	0.387	−1.159	2.600	0.123	0.287
0.04	−0.845	0.371	−1.187	2.692	0.137	0.304
0.05	−0.724	0.360	−1.199	2.664	0.140	0.304
0.06	−0.622	0.351	−1.191	2.733	0.122	0.309
0.07	−0.550	0.347	−1.188	2.980	0.100	0.310
0.08	−0.486	0.347	−1.204	3.210	0.086	0.328
0.09	−0.442	0.347	−1.214	3.176	0.089	0.321

Table 2 continued

T	b_1	b_2	b_3	b_4	b_5	σ
0.10	−0.442	0.349	−1.217	2.950	0.101	0.329
0.20	−0.715	0.369	−1.058	2.211	0.111	0.312
0.31	−1.248	0.464	−1.161	2.545	0.115	0.293
0.40	−1.451	0.492	−1.172	3.015	0.099	0.292
0.51	−1.640	0.517	−1.196	2.604	0.087	0.295
0.62	−1.827	0.540	−1.214	2.279	0.075	0.292
0.70	−1.977	0.554	−1.209	2.169	0.060	0.302
0.80	−2.152	0.572	−1.192	2.062	0.036	0.288
0.90	−2.354	0.592	−1.165	1.966	−0.001	0.286
1.03	−2.572	0.617	−1.151	1.822	−0.034	0.286
1.17	−2.795	0.647	−1.171	1.698	−0.038	0.290
1.24	−2.927	0.666	−1.186	1.683	−0.037	0.284
1.32	−3.066	0.686	−1.203	1.676	−0.039	0.272
1.41	−3.215	0.707	−1.215	1.658	−0.050	0.263
1.50	−3.363	0.726	−1.222	1.618	−0.070	0.266
1.60	−3.508	0.745	−1.224	1.580	−0.098	0.270
1.71	−3.643	0.761	−1.225	1.547	−0.133	0.275
1.82	−3.759	0.773	−1.219	1.486	−0.172	0.286
1.94	−3.874	0.784	−1.213	1.444	−0.203	0.295
2.07	−3.981	0.793	−1.204	1.404	−0.234	0.300
2.20	−4.080	0.801	−1.194	1.368	−0.263	0.302
2.35	−4.170	0.806	−1.181	1.334	−0.293	0.313
2.50	−4.253	0.809	−1.166	1.303	−0.321	0.324

Table 3 Model parameters for inelastic system with ductility 1.5

T	b_1	b_2	b_3	b_4	b_5	σ
0.04	−0.959	0.378	−1.171	2.666	0.134	0.295
0.05	−0.911	0.372	−1.172	2.672	0.138	0.297
0.06	−0.842	0.364	−1.161	2.739	0.123	0.295
0.07	−0.765	0.358	−1.167	2.930	0.108	0.298
0.08	−0.710	0.358	−1.184	3.117	0.097	0.309
0.09	−0.683	0.359	−1.194	3.115	0.098	0.303
0.10	−0.688	0.360	−1.193	2.938	0.105	0.309
0.20	−1.008	0.396	−1.099	2.404	0.105	0.299
0.31	−1.447	0.464	−1.144	2.696	0.108	0.284
0.40	−1.591	0.482	−1.162	2.756	0.097	0.286
0.51	−1.848	0.521	−1.199	2.554	0.062	0.287
0.62	−2.001	0.538	−1.215	2.368	0.050	0.286
0.70	−2.167	0.556	−1.214	2.169	0.047	0.292
0.80	−2.379	0.578	−1.199	2.003	0.030	0.277

Table 3 continued

T	b_1	b_2	b_3	b_4	b_5	σ
0.90	−2.605	0.602	−1.176	1.848	−0.005	0.269
1.03	−2.796	0.623	−1.163	1.691	−0.032	0.282
1.17	−2.986	0.646	−1.178	1.590	−0.036	0.275
1.24	−3.101	0.661	−1.191	1.555	−0.035	0.272
1.32	−3.218	0.677	−1.204	1.541	−0.042	0.261
1.41	−3.352	0.695	−1.216	1.544	−0.053	0.256
1.50	−3.510	0.717	−1.224	1.540	−0.069	0.262
1.60	−3.667	0.738	−1.227	1.507	−0.099	0.266
1.71	−3.796	0.754	−1.229	1.502	−0.134	0.276
1.82	−3.923	0.769	−1.226	1.487	−0.175	0.288
1.94	−4.047	0.781	−1.217	1.483	−0.203	0.295
2.07	−4.167	0.791	−1.204	1.483	−0.229	0.295
2.20	−4.282	0.800	−1.187	1.488	−0.253	0.306
2.35	−4.391	0.806	−1.167	1.497	−0.275	0.307
2.50	−4.495	0.811	−1.142	1.510	−0.294	0.309

Table 4 Model parameters for inelastic system with ductility 2

T	b_1	b_2	b_3	b_4	b_5	σ
0.04	−1.000	0.381	−1.167	2.728	0.135	0.289
0.05	−0.973	0.376	−1.166	2.777	0.139	0.293
0.06	−0.924	0.370	−1.158	2.825	0.123	0.288
0.07	−0.867	0.366	−1.161	2.951	0.109	0.296
0.08	−0.833	0.367	−1.173	3.079	0.101	0.302
0.09	−0.820	0.367	−1.179	3.031	0.106	0.293
0.10	−0.845	0.371	−1.179	2.883	0.113	0.300
0.20	−1.183	0.413	−1.121	2.395	0.102	0.299
0.31	−1.592	0.471	−1.142	2.797	0.098	0.276
0.40	−1.720	0.483	−1.151	2.628	0.096	0.283
0.51	−2.020	0.527	−1.188	2.614	0.055	0.280
0.62	−2.210	0.548	−1.195	2.435	0.033	0.281
0.70	−2.317	0.557	−1.190	2.197	0.025	0.273
0.80	−2.490	0.573	−1.175	1.881	0.012	0.268
0.90	−2.717	0.601	−1.172	1.734	−0.010	0.279
1.03	−2.925	0.628	−1.188	1.632	−0.032	0.270
1.17	−3.122	0.653	−1.210	1.560	−0.047	0.250
1.24	−3.226	0.667	−1.222	1.528	−0.056	0.256
1.32	−3.343	0.682	−1.232	1.471	−0.067	0.264
1.41	−3.494	0.702	−1.238	1.456	−0.082	0.264
1.50	−3.682	0.727	−1.238	1.466	−0.104	0.270
1.60	−3.848	0.747	−1.231	1.481	−0.133	0.278

Table 4 continued

T	b_1	b_2	b_3	b_4	b_5	σ
1.71	−3.985	0.763	−1.224	1.504	−0.172	0.281
1.82	−4.101	0.774	−1.210	1.517	−0.203	0.287
1.94	−4.221	0.784	−1.196	1.521	−0.223	0.288
2.07	−4.332	0.792	−1.179	1.523	−0.239	0.298
2.20	−4.433	0.797	−1.159	1.524	−0.251	0.300
2.35	−4.524	0.800	−1.137	1.522	−0.258	0.303
2.50	−4.605	0.800	−1.111	1.520	−0.262	0.307

Table 5 Model parameters for inelastic system with ductility 4

T	b_1	b_2	b_3	b_4	b_5	σ
0.04	−1.084	0.388	−1.158	2.694	0.132	0.283
0.05	−1.104	0.387	−1.155	2.726	0.134	0.286
0.06	−1.075	0.382	−1.155	2.800	0.128	0.283
0.07	−1.049	0.380	−1.159	2.885	0.123	0.290
0.08	−1.039	0.381	−1.165	2.941	0.122	0.286
0.09	−1.056	0.383	−1.164	2.896	0.122	0.281
0.10	−1.075	0.386	−1.167	2.845	0.126	0.281
0.20	−1.554	0.449	−1.153	2.475	0.096	0.284
0.31	−1.851	0.483	−1.155	2.765	0.102	0.267
0.40	−2.098	0.512	−1.172	2.565	0.068	0.278
0.51	−2.350	0.546	−1.205	2.482	0.043	0.273
0.62	−2.583	0.570	−1.188	2.271	0.016	0.268
0.70	−2.780	0.588	−1.160	1.967	−0.008	0.261
0.80	−3.002	0.610	−1.139	1.795	−0.028	0.266
0.90	−3.208	0.636	−1.154	1.840	−0.052	0.269
1.03	−3.405	0.664	−1.186	1.926	−0.079	0.276
1.17	−3.627	0.695	−1.213	1.933	−0.111	0.270
1.24	−3.747	0.709	−1.216	1.914	−0.131	0.270
1.32	−3.894	0.727	−1.215	1.902	−0.150	0.273
1.41	−4.052	0.746	−1.209	1.886	−0.168	0.272
1.50	−4.204	0.760	−1.192	1.857	−0.183	0.269
1.60	−4.333	0.771	−1.173	1.827	−0.198	0.272
1.71	−4.439	0.778	−1.152	1.771	−0.212	0.272
1.82	−4.537	0.783	−1.132	1.689	−0.225	0.283
1.94	−4.654	0.792	−1.113	1.579	−0.239	0.286
2.07	−4.773	0.800	−1.093	1.446	−0.253	0.296
2.20	−4.892	0.808	−1.073	1.290	−0.267	0.306
2.35	−5.012	0.817	−1.052	1.110	−0.282	0.315
2.50	−5.132	0.825	−1.032	0.907	−0.297	0.325

References

Abrahamson NA, Silva WJ (1997) Empirical response spectral attenuation relations for shallow crustal earthquakes. Seismol Res Lett 68(1):94–127

Ambraseys NN, Bommer JJ (1991) The attenuation of ground accelerations in Europe. Earthq Eng Struct Dyn 20(12):1179–1202. doi:10.1002/eqe.4290201207

Ambraseys NN, Simpson KA, Bommer JJ (1996) Prediction of horizontal response spectra in Europe. Earthq Eng Struct Dyn 25(4):371–400. doi:10.1002/(SICI)1096-9845(199604)25:4<371::AID-EQE550>3.0.CO;2-A

Ambraseys NN, Smit P, Douglas J, Margaris B, Sigbjörnsson R, Olfasson S, Suhadolc P, Costa G (2004a) Internet site for European strong-motion data. Boll Geofisica Teorica Applicata 45:113–129

Ambraseys NN, Douglas J, Sigbjörnsson R, Berge-Thierry C, Suhadolc P, Costa G (2004b) European strong-motion database (vol 2). Imperial College, London

Ambraseys NN, Douglas J, Sharma SK, Smit PM (2005) Equations for the estimation of strong ground motions from shallow crustal earthquakes using data from Europe and the Middle East: horizontal peak ground acceleration and spectral acceleration. Bull Earthq Eng 3(1):1–53. doi:10.1007/s10518-005-0183-0

Berge-Thierry C, Cotton F, Scotti O, Griot-Pommera D, Fukushima Y (2003) New empirical response spectral attenuation laws for moderate European earthquakes. J Earthq Eng 7(2):193–222. doi:10.1142/S1363246903001061

Bertero V (1997) Performance-based seismic engineering: a critical review of proposed guidelines. In: Fajfar P, Krawinkler HSeismic design methodologies for the next generation of codes. AA Balkema, Rotterdam pp 1–31

Bindi D, Luzi L, Pacor F, Franceshina G, Castro RR (2006) Ground-motion predictions from empirical attenuation relationships versus recorded data: the case of the 1997–1998 Umbria-Marche, central Italy, strong-motion data set. Bull Seismol Soc Am 96(3):984–1002. doi:10.1785/0120050102

Biot MA (1942) Analytical and experimental methods in engineering seismology. ASCE Trans 5:365–408

Bommer JJ, Elnashai AS, Chlimintzas GO, Lee D (1998) Review and development of response spectra for displacement-based seismic design. ESEE Research Report No. 98-3, ICONS. Imperial College, London

Boore DM, Joyner WB, Fumal TE (1997) Equations for estimating horizontal response spectra and peak acceleration from western North American earthquakes: a summary of recent work. Seismol Res Lett 68(1):128–153

Borzi B, Calvi GM, Elnashai AS, Faccioli E, Bommer JJ (2001) Inelastic spectra for displacement-based seismic design. Soil Dyn Earthq Eng 21:47–61. doi:10.1016/S0267-7261(00)00075-0

Cauzzi C, Faccioli E (2008) Broadband (0.05–20 s) prediction of displacement response spectra based on worldwide digital records. J Seismol 12:453–475. doi 10.1007/s10950-008-9098-y

Cornell CA (1968) Engineering seismic risk analysis. Bull Seismol Soc Am 58:1583–1606

Douglas J (2003) Earthquake ground motion estimation using strong-motion records: a review of equations for the estimation of peak ground acceleration and response spectral ordinates. Earth Sci Rev 61(1–2):43–104. doi:10.1016/S0012-8252(02)00112-5

European Committee for Standardization (2003) Eurocode 8: design of structures for earthquake resistance-Part1: general rules, seismic actions and rules for buildings, European Standard

Frankel A, McGarr A, Bicknell J, Mori J, Seeber L, Cranswick E (1990) Attenuation of high frequency shear waves in the crust: measurements from New York State, South Africa, and southern California. J Geophys Res 95(B11):17441–17457. doi:10.1029/JB095iB11p17441

Hachem MM (2000) Bispec help manual. http://www.ce.berkeley.edu/~hachem/BispecHelp

Hachem MM (2008) Bispec version 1.61. http://www.ce.berkeley.edu/~hachem/bispec

Housner GW (1959) Behaviour of structures during earthquakes. J Eng Mech Div 85:109–129

Joyner WB, Boore DM (1981) Peak horizontal acceleration and velocity from strong-motion records including records from the 1979 Imperial Valley, California, earthquake. Bull Seismol Soc Am 71(6):2011–2038

Kanamori H (1977) The energy release in great earthquakes. J Geophys Res 82(20):2981–2987. doi:10.1029/JB082i020p02981

Kowalsky MJ, Priestley MJN, MacRae GA (1994) Displacement-based design, a methodology for seismic design applied to sdof reinforced concrete structures. Report No. SSRP-94/16, Structural system research project, University of California, San Diego, La Jolla, CA.

McGuire RK (1977) Seismic design spectra and mapping procedures using hazard based directly on oscillator response. Earthq Eng Struct Dyn 5(3):211–234. doi:10.1002/eqe.4290050302

Moehle JP (1992) Displacement-based design of R/C structures subjected to earthquakes. Earthq Spectra 8(3):403–427. doi:10.1193/1.1585688

Mohraz B (1976) A study of earthquake response spectra for different geological conditions. Bull Seismol Soc Am 66:915–935

Newmark NM, Hall WJ (1969) Seismic design criteria for nuclear reactor facilities. Proceedings of the 4th World conference on earthquake engineering B-4:37–50
Priestley MJN (2000) Performance based seismic design. Bull N Z Soc Earthq Eng 33(3):325–346
Priestley MJN, Calvi GM, Kowalsky MJ (2007) Displacement based seismic design of structures. IUSS press, Pavia Italy
Savitzky A, Golay MJE (1964) Smoothing and differentiation of data by simplified least squares procedures. Anal Chem 36:1627–1639. doi:10.1021/ac60214a047
Seed HB, Ugas C, Lysmer J (1976) Site-dependent spectra for earthquake resistant design. Bull Seismol Soc Am 66:221–243
SeismoSignal (2007) ver.3.2.0, http://www.seismosoft.com
Sigbjörnsson R, Ólafsson S (2004) On the south Iceland earthquakes in June 2000: strong-motion effects and damage. Boll Geofisica Teorica Applicata 45(3):131–152
Sigbjörnsson R, Ólafsson S, Snæbjörnsson J (2007) Macroseismic effects related to strong ground motion: a study of the South Iceland earthquakes in June 2000. Bull Earthq Eng 5:591–608. doi:10.1007/s10518-007-9045-2
Sigbjörnsson R, Snæbjörnsson J, Higgins S, Halldórsson B (2008) A note on the Mw 6.3 earthquake in Iceland on 29 May 2008 at 15:45 UTC. Bull Earthq Eng. doi:10.1007/s10518-008-9087-0
Tothong P, Cornell CA (2006) An empirical ground motion attenuation relation for inelastic spectral displacement. Bull Seismol Soc Am 96(6):2146–2164. doi:10.1785/0120060018
Trifunac MD (1992) Should peak acceleration be used to scale design spectral amplitudes? Proceedings of the 10th World conference on earthquake engineering, Madrid, Spain. 10:5817–5822